

Hybrid turbidite-drift channel complexes: An integrated multiscale model

A. Fuhrmann¹, I.A. Kane¹, M.A. Clare², R.A. Ferguson¹, E. Schomacker³, E. Bonamini⁴ and F.A. Contreras⁵

¹Department of Earth and Environmental Sciences, University of Manchester, Williamson Building, Oxford Road, Manchester M13 9PL, UK

²National Oceanography Centre, European Way, Southampton SO14 3HZ, UK

³Equinor, Martin Linges vei 33, 1364 Fornebu, Norway

⁴Eni Upstream and Technical Services, Via Emilia 1, 20097 San Donato Milanese, Milan, Italy

⁵Eni Rovuma Basin, no. 918, Rua dos Desportistas, Maputo, Mozambique

ABSTRACT

The interaction of deep-marine bottom currents with episodic, unsteady sediment gravity flows affects global sediment transport, forms climate archives, and controls the evolution of continental slopes. Despite their importance, contradictory hypotheses for reconstructing past flow regimes have arisen from a paucity of studies and the lack of direct monitoring of such hybrid systems. Here, we address this controversy by analyzing deposits, high-resolution sea-floor data, and near-bed current measurements from two sites where eastward-flowing gravity flows interact(ed) with northward-flowing bottom currents. Extensive seismic and core data from offshore Tanzania reveal a 1650-m-thick asymmetric hybrid channel levee-drift system, deposited over a period of ~20 m.y. (Upper Cretaceous to Paleocene). High-resolution modern seafloor data from offshore Mozambique reveal similar asymmetric channel geometries, which are related to northward-flowing near-bed currents with measured velocities of up to 1.4 m/s. Higher sediment accumulation occurs on the downstream flank of channel margins (with respect to bottom currents), with inhibited deposition or scouring on the upstream flank (where velocities are highest). Toes of the drift deposits, consisting of thick laminated muddy siltstone, which progressively step back into the channel axis over time, result in an interfingering relationship with the sandstone-dominated channel fill. Bottom-current flow directions contrast with those of previous models, which lacked direct current measurements or paleoflow indicators. We finally show how large-scale depositional architecture is built through the temporally variable coupling of these two globally important sediment transport processes. Our findings enable more-robust reconstructions of past oceanic circulation and diagnosis of ancient hybrid turbidite-drift systems.

INTRODUCTION

As the terminal part of sedimentary source-to-sink systems, deep-sea deposits have been used to reconstruct past climates, sediment and carbon budgets, and the distribution of anthropogenic pollution (Sømme et al., 2009; Masson et al., 2010; Rebesco et al., 2014; Drinkorn et al., 2019; Kane and Clare, 2019). Bottom currents, i.e., density-driven circulation in the deep ocean, and sediment gravity flows are the main processes that form and modify these deposits (e.g., Talling et al., 2012; Rebesco et al., 2014). While the influence of bottom currents on submarine channel architecture has been recognized, interpretation has been hampered by a lack of direct monitoring data (Shanmugam et al., 1993;

Gong et al., 2018; Sansom, 2018; Fonesu et al., 2020). Modern, integrated data sets, including direct measurements and monitoring of bottom currents, are of great importance in understanding the complexity of oceanographic processes (Fierens et al., 2019; Miramontes et al., 2019; Thiéblemont et al., 2019), sediment gravity flows (Clare et al., 2016; Azpiroz-Zabala et al., 2017; Symons et al., 2017), and the preservation of strata within submarine channel complexes (Gamberi et al., 2013; Vendettuoli et al., 2019). This study combines an integrated subsurface study (three-dimensional [3-D] seismic, core, and well-log data) with modern seafloor geomorphology and near-bed bottom-current measurements to develop a process-product-based

sedimentological model for bottom current-influenced submarine channel complexes.

GEOLOGICAL SETTING

The Jurassic to Paleogene basins offshore of East Africa formed during the breakup of Gondwana (Salman and Abdula, 1995). Following Pliensbachian to Aalenian northwest-southeast rifting, ~2000 km of continental drift took place along north-south-striking lineaments, such as the Davie Ridge fracture zone (DFZ) and the Sea Gap fault (SGF) (Fig. 1A), between the Kimmeridgian and Barremian (Reeves, 2018) (Fig. 1B). Cessation of rifting was marked by active seafloor spreading between Madagascar and India, leading to the development of the present-day East African passive continental margin (Reeves et al., 2016). Albian transgression resulted in the development of the extensive deep-marine deposits that are the focus of this study. Major river systems drained the African continent and supplied fine-grained sediment, while additional sediment was shed from uplifted rift shoulders along the paleocoastline (Smelror et al., 2008; Fossum et al., 2019).

DATA AND METHODS

This study used high-resolution 3-D seismic reflection data (covering 4885 km²) and 14 exploration wells provided by Equinor ASA (Norway) and ExxonMobil (USA). Seismic data were tied to the biostratigraphically calibrated wells (and core data of Well A; Figs. 1C and 1D) to map seismic and stratigraphic geometries offshore Tanzania (Fig. 1). The average vertical resolution in the Upper Cretaceous of our study area is ~20–30 m (average velocities of ~2.9–3.3 km/s, and average frequency of 35 Hz). The data have a bin spacing of 12.5 × 12.5 m and a

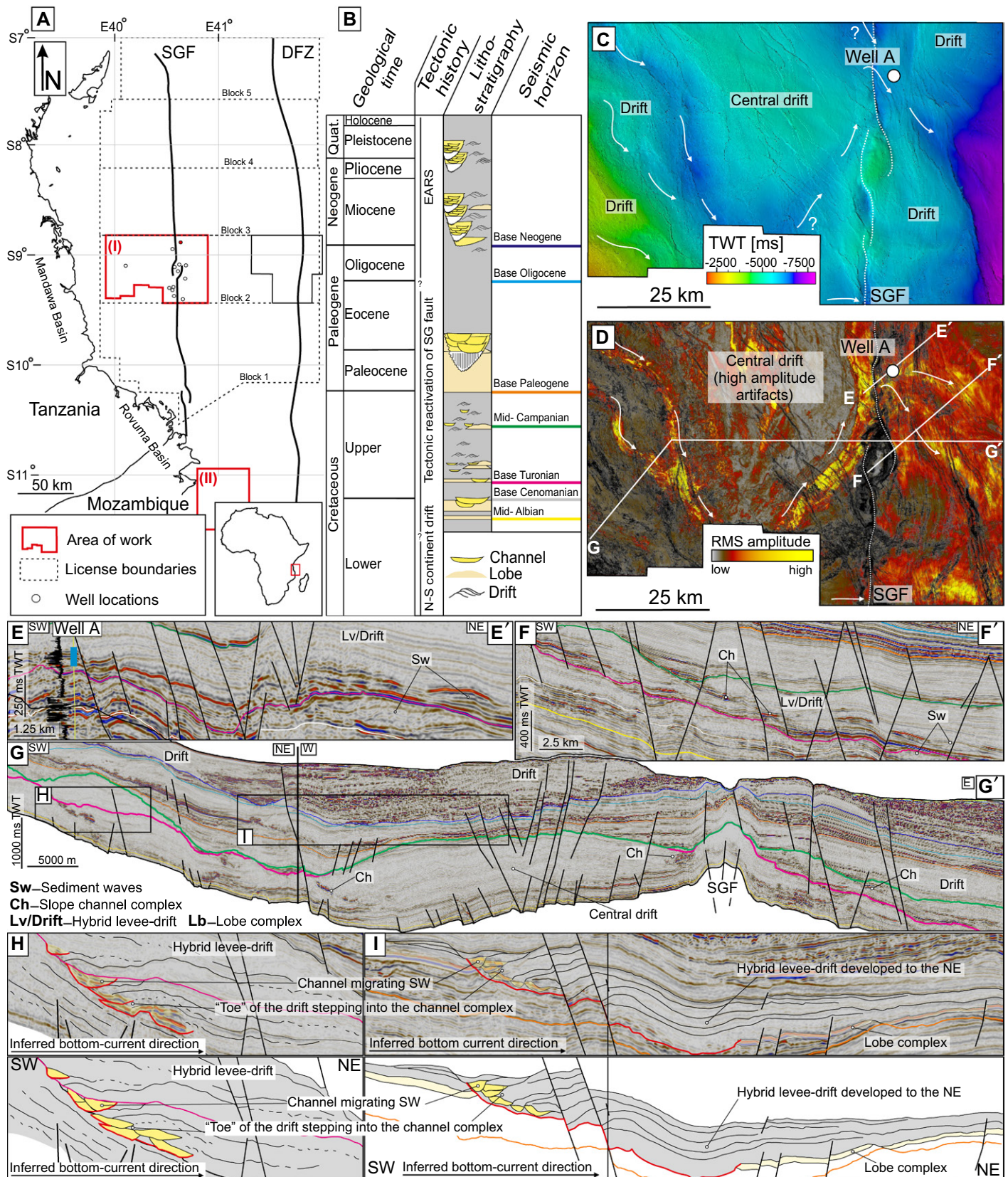


Figure 1. (A) Location of the subsurface data (red outline I) and modern analogue (red outline II), the Sea Gap Fault (SGF) and the Davie Ridge Fracture Zone (DFZ) along the East African Margin. Dotted lines refer to regional oil/gas license boundaries. Wells were used for biostratigraphic correlation; Well A is marked by red dot. (B) Lithology and tectonic history of the deep-water basins offshore of Tanzania. Colors of seismic horizons correlate to the interpreted seismic cross sections in panels E–I. Quat—Quaternary; EARS—East African Rift System. (C,D) Contour map of mid-Campanian (C) seismic horizon and root mean square (RMS) amplitude extraction of the base Turonian to mid-Campanian (D). Coarse-grained sediment (high amplitudes) is influenced by drift-related topography (low amplitudes); white arrows mark direction of sediment gravity flows. TWT—two-way travelttime. (E) Seismic cross section showing Well A (blue line; well tie is shown in Fig. 3C) and lateral seismic facies

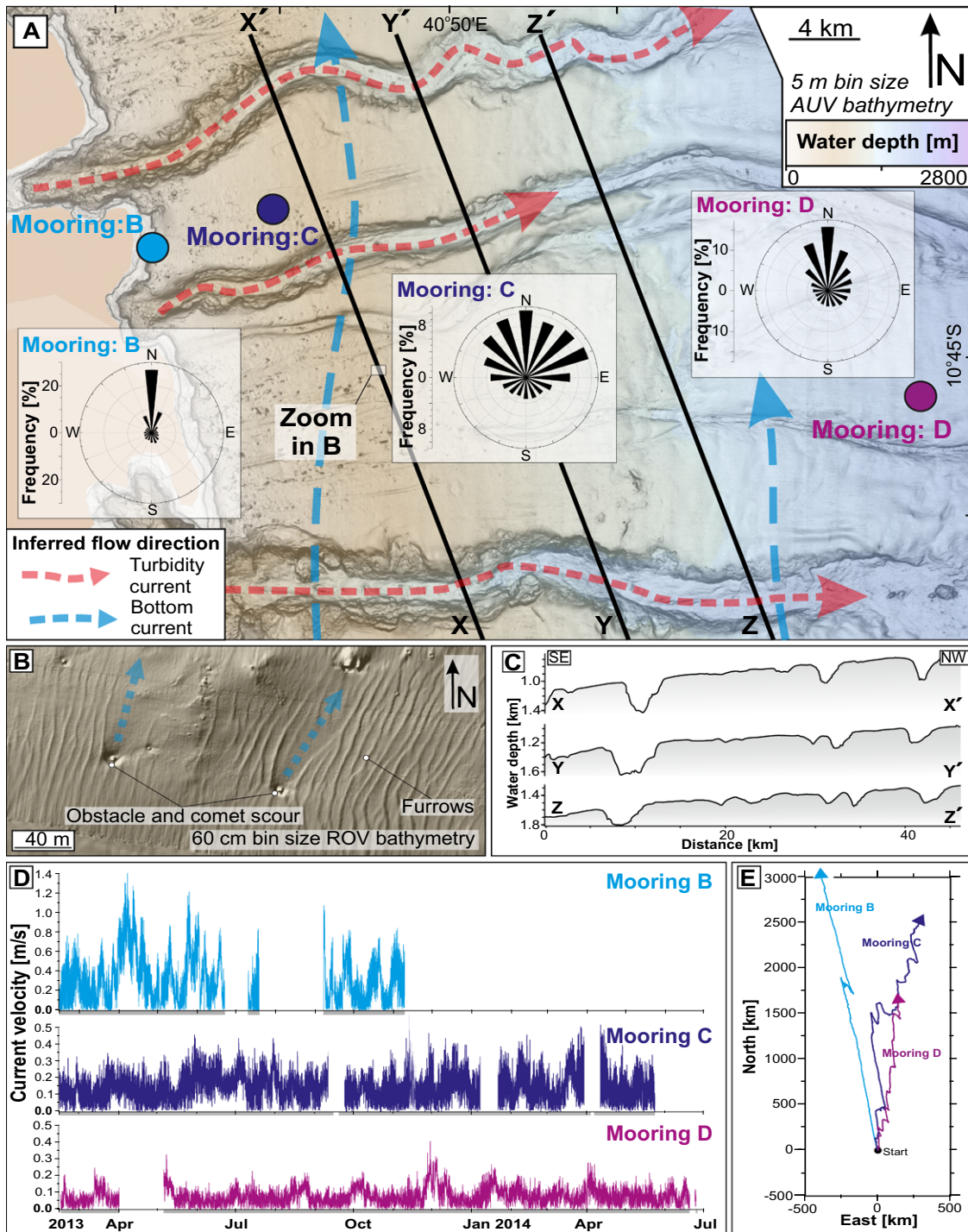


Figure 2. Modern bottom-current and seafloor data, offshore northern Mozambique. (A) Bathymetric map of the seafloor including location of moorings and cross sections. AUV—autonomous underwater vehicle. (B) Furrows and scours at the seafloor indicate the dominance of north-flowing bottom currents. ROV—remotely operated vehicle. (C) Cross sections X, Y, and Z showing less-steep canyon walls (drift) at the northern flank of canyons. (D) Bottom-current velocity measurements for each mooring indicate strong seasonal variability. Gray bars on time axis represent times in which data were recorded. (E) Cumulative vector plot shows dominant trend of currents flowing to north.

4 ms sampling rate, and are processed in the Society of Exploration Geophysicists (SEG) normal polarity to zero phase, where a peak variation. (F) Seismic cross section showing drift-confined slope channels and sediment waves east of Sea Gap fault. (G) Seismic cross section displaying spatial distribution of drift deposits and Sea Gap fault. (H,I) Zoom of hybrid levee-drift deposits in Upper Cretaceous and Paleogene (top) with interpretation (bottom). Note overall similar trend of coeval channel and drift migration.

(yellow in Figs. 1E–1I) represents a downward increase in acoustic impedance. High-resolution modern seafloor data covering the modern analog, offshore northern Mozambique, comprises extensive (65 × 50 km) multibeam bathymetric data acquired by our study using an autonomous underwater vehicle (5 m bin size), and a focused (190-m-wide) bathymetric survey using a remotely operated vehicle (0.6 m bin size; Fig. 2). Down-looking 1200 kHz acoustic Doppler current profilers (ADCPs) deployed by Eni energy company on three single-point deep-water

moorings (moorings B, C, and D in Fig. 2A) measured near-bed (5.5 m above bed) current direction and velocity every 10 min from March 2013 to September 2014 (Figs. 2D and 2E).

SEISMIC EVIDENCE FOR DOWN- AND ALONG-SLOPE SEDIMENT TRANSPORT

The deep-marine sedimentary systems of the Upper Cretaceous offshore Tanzania were strongly influenced by topographic relief associated with the Sea Gap fault and large drift

deposits (Figs. 1C, 1D, and 1G). These drifts are characterized by low-amplitude, parallel to wavy reflectors, which show a lateral, upslope accretion toward the southwest. A 1650-m-thick drift (central drift) with horizontal dimensions that exceed the data coverage of the 3-D seismic survey toward the north (maximum west-east width of 50 km) dominates the stratigraphy (Figs. 1C, 1D, and 1G). Smaller drifts as much as 12 km wide and 30 km long, to the west of the central drift, migrated obliquely along the northwest-southeast-oriented upper slope. Located in their topographic lows are concave-up, ~3500-m-wide high-amplitude reflectors, interpreted as coarse-grained submarine slope channel fills (Figs. 1E, 1F, 1H, and 1I). These drifts show characteristics of levees, developed on the northeastern side of the channel complexes, and migrated up dip (southwest), confining and stepping into the channels. One-sided hybrid levee-drift deposits on the northeastern sides of channel systems are recognized from the Upper Cretaceous to modern systems (Fig. 1G). East of the Sea Gap fault, large drifts, low-amplitude sediment waves (wavelengths ~1.5–2.5 km, ~100 m thick), and distal slope channel complexes indicate similar channel and drift interaction along the lower slope (Figs. 1E and 1F). The time-continuous migration toward the southwest, the low seismic amplitude of the drifts, and the dimming of high-amplitude channel fills to the north suggest relatively persistent, long-lived bottom-current flow (Faugères et al., 1999).

MODERN-DAY SEAFLOOR OBSERVATIONS AND CURRENT MEASUREMENTS

Acoustic Doppler current profiler measurements offshore of Mozambique show a dominance of northward-directed bottom currents (Fig. 2), which typically attain near-bed velocities between 0.2 and 0.4 m/s, with a maximum of 1.4 m/s (Fig. 2D). Cumulative vector plots of each deep-water mooring calculated from the current speed and duration show the northward transport of the near-bed water masses along the entire slope (Fig. 2E). These currents are likely related to the East African Coastal Current (moorings B and D) and deeper Antarctic Intermediate Water (Schouten et al., 2003; van Aken et al., 2004; Thiéblemont et al., 2019). Annual variation in current strength may relate to the seasonal occurrence of eddies along the Mozambique Channel (de Ruijter et al., 2002; Nauw et al., 2008; Miramontes, et al., 2019; Thiéblemont et al., 2019). Bathymetric observations of north- to north-northeast-oriented obstacle-scour features and linear furrows (Fig. 2B) match the measured current direction from ADCPs, and indicate bottom-current velocities of ~0.2–1.0 m/s, according to Stow et al. (2009). The rounded, less-steep northern

channel flanks are interpreted as drifts stepping into the channels (Fig. 2C).

BED-SCALE OBSERVATIONS ACROSS HYBRID SYSTEMS

Well A intersects high-amplitude, sandstone-dominated channel fills (Figs. 1D and 1E). These high amplitudes decay toward the northeast, where they interfinger with low amplitudes of muddier drift deposits. The gamma-ray log (Fig. 3C) shows repetitive low-intensity intervals that grade into spiky well-log responses, interpreted as coarse-grained sandstone packages that fine upward into mud-prone heterolithic sediments. Core facies are dominated by (1) turbidites, with lesser debrites and hybrid event beds (facies Fa1–Fa4; Figs. 3A and 3B; Table DR1 in the GSA Data Repository¹); (2) muddy siltstones interbedded with 5–10-cm-thick, sharp-based sandstones grading into mottled siltstone with starved ripples and laminae, interpreted as reworked low-density turbidites (facies Fa5; Fig. 3B) (e.g., Shanmugam et al., 1993; Martín-Chivelet et al., 2008); and (3) muddy siltstones, 0.5–2 m thick, with parallel lamination, rare cross-cutting laminae, and ripples, interpreted as bottom-current deposits (facies Fa6; Fig. 3B). The well-sorted, narrow grain-size range of facies Fa6 suggests relatively weak, but long-lasting, flow. Individual cross-cutting laminae that are overlain by ripples indicate short-term increases in bottom-current strength and erosion (Fig. 3B). The limited occurrence of normal and inverse grading, well-preserved primary sedimentary structures, and relatively uniform grain size distinguish these deposits from those of other contourite facies models (e.g., Stow and Faugères, 2008). The removal of organic matter in combination with high silt sedimentation rates could account for the suppression of bioturbation and the preservation of primary sedimentary structures.

A MODEL FOR TEMPORALLY VARIABLE BOTTOM-CURRENT INTERACTION WITH SUBMARINE CHANNELS

To understand the interaction of sediment gravity flows and bottom currents, it is important to consider these processes in terms of their orientation, thickness, velocity, steadiness, and persistence over time. Our model (Fig. 4) is based on geometries and facies stacking patterns considered to be representative of strong (i.e.,

velocities of meters per second), short-duration (minutes to days), unsteady, episodic turbidity currents, and relatively weak (i.e., velocities of centimeters per second) but quasi-steady bottom currents (over geological time scales) (Fig. 4C). For turbidity flows, velocity values were collated from recent monitoring studies (Table DR2), while a compilation of published bottom-current velocity data augments our own measurements from offshore Mozambique (Table DR3). Bottom-current velocity typically fluctuates annually, with average recorded velocities in the region of 0.4 m/s and short-lived peaks of up to 1.4 m/s; flows of these velocities are able to entrain and redistribute the silt- and sand-grade sediment deposited by turbidity currents (Stow et al., 2009, and references therein).

When sediment gravity flow systems are active (Fig. 4Ai), the channels undergo cycles of erosion, bypass, and deposition under unsteady flow conditions (*sensu* Hubbard et al., 2014). Thick, amalgamated, high-density turbidites are deposited in the channel axis, laterally changing into individual turbidite beds with preserved bed tops in channel off-axis positions (facies Fa1 and Fa2). Direct interaction of turbidity currents and northward-flowing bottom currents is short lived, but is anticipated to result in partial flow-stripping of the super-elevated fraction of turbidity currents (Shanmugam et al., 1993). For the majority of the time, sediment gravity flows are subordinate to the north-flowing bottom currents (Fig. 4Aii). During this time, the channel and levee deposits are reworked and redistributed, forming one-sided, hybrid levee-drift deposits to the north (*sensu* Shanmugam et al., 1993; Palermo et al., 2014; Sansom, 2018; Fonescu et al., 2020). Deceleration and partial deflection of bottom currents interacting with the topography of the channel cause high accretion rates on the upstream-facing channel flank (relative to the bottom current) under lee-wave conditions (Flood, 1988). Thick homogeneous muddy siltstones (facies Fa6) deposited by bottom currents step into the channel and ultimately interfinger with the channel margin (facies Fa1 and Fa2; Fig. 3A) and reworked overbank and/or levee facies (facies Fa5; Fig. 3). For this reason, there is minimal levee development on the bottom current-upstream side of the channel (cf. Gong et al. 2018). Sedimentary facies and architecture of the hybrid turbidite-drift channel systems are therefore controlled by the frequency of sediment gravity flow activity and the relative persistence and strength of bottom currents. Deposit modification would mostly occur during periods when bottom currents dominate; during this time, the strength and character or direction of the bottom current system would be variable due to, for example, seasonal eddies and benthic storms (Thran et al., 2018; Miramontes, et al., 2019). However, changes in sediment flux (i.e., frequency of sediment gravity flows) and fluctuation of bottom currents over geological time scales (10⁶ m.y.) govern

¹GSA Data Repository item 2020157, Table DR1 (facies), Table DR2 (published deep-ocean turbidity current measurements), and Table DR3 (published near-bed bottom current measurements), is available online at <http://www.geosociety.org/datarepository/2020/>, or on request from editing@geosociety.org. Cumulative bottom-current vector data from offshore Mozambique are available at <https://doi.org/10.6084/m9.figshare.11708490>.

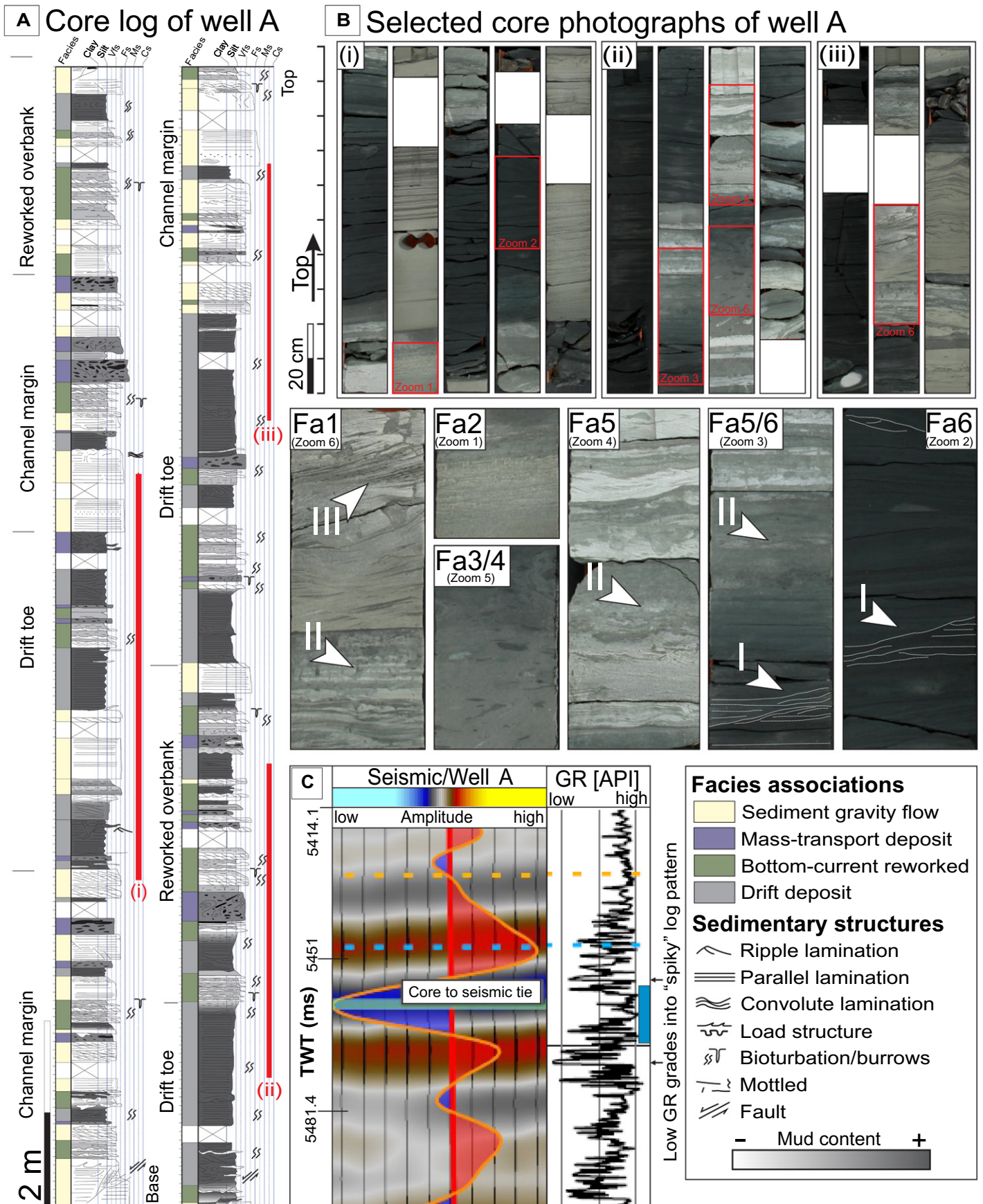
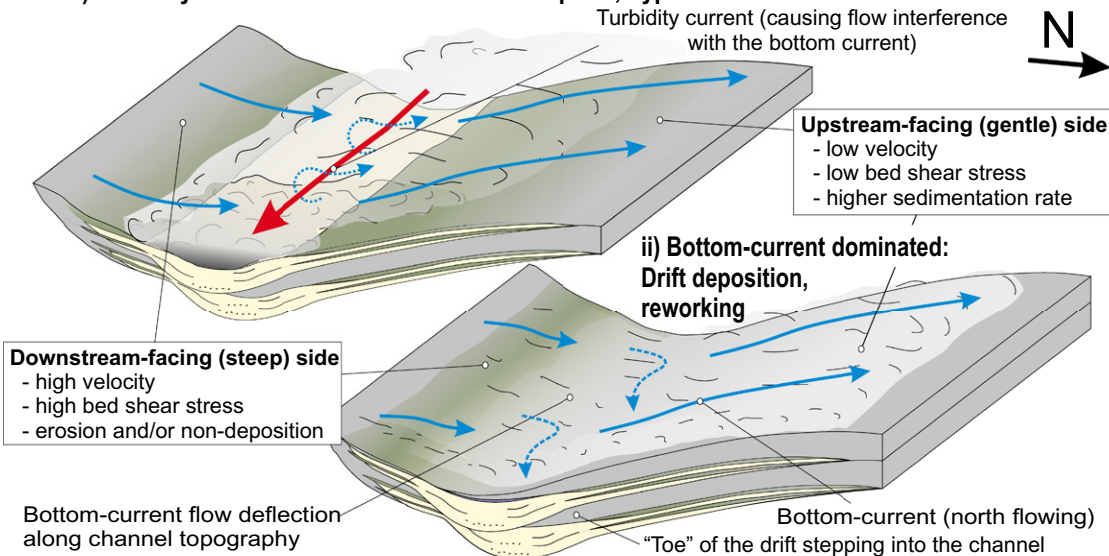


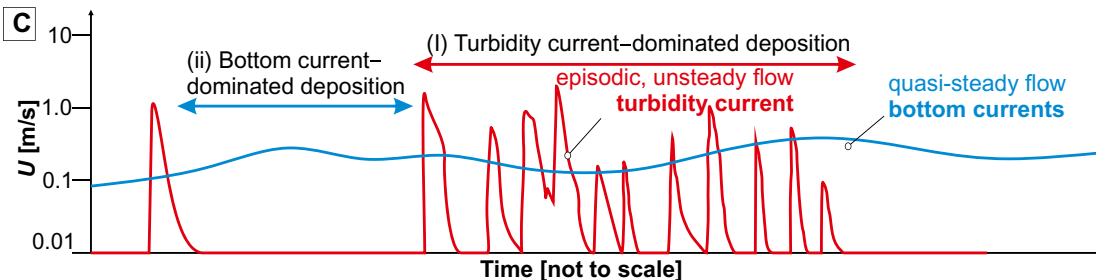
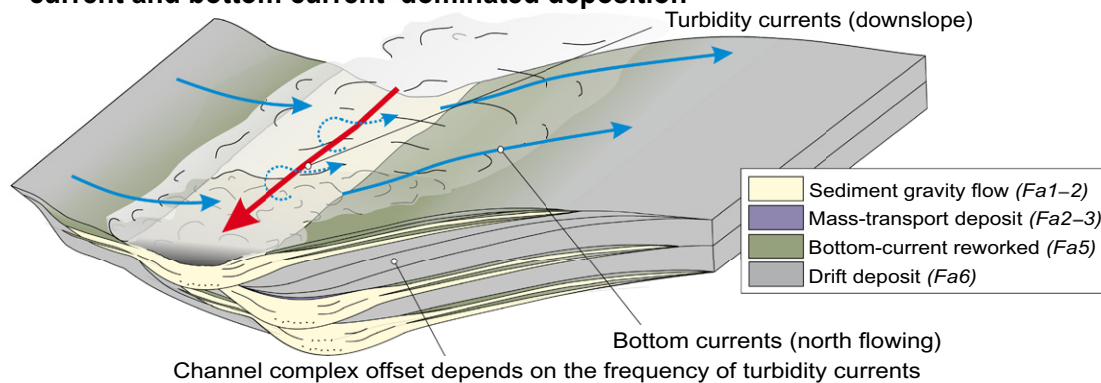
Figure 3. (A) Sedimentological log of Well A, offshore Tanzania (see Fig. 1A). Vfs—very fine sand; Fs—fine sand; Ms—medium sand; Cs—coarse sand. (B) Well A core photographs: i—drift deposits interbedded with turbidites; ii—reworked turbidites interbedded with toes of drift; iii—drift facies transitioning into muddy turbidites. Zoom on individual facies associations (Fa): Fa6—drift deposit with parallel, cross-cutting

A Process-based model of channelized turbidity- and bottom currents

i) Turbidity current dominated: Channel inception, bypass and infill



B Laterally offset channel complexes after repetitive interaction of turbidity-current and bottom current-dominated deposition



and ripple-laminated muddy siltstone (I); Fa5—coarsening up into sharp-based thin low density turbidites (LDTs) with starved ripple lamination and bioturbated bed tops (II); Fa1—LDT, including muddy cross-lamination (III) and muddy climbing ripple lamination (II); Fa2—transitional flow deposits; Fa3—debrite; Fa4—slumped deposits. (C) Well A to seismic tie shows seismic amplitudes in the background with the correlated wiggles along the well path (red line). Seismic pick D represents a tie point between seismic and well; dotted lines are seismic horizons; blue bar represents the cored interval (A). GR—gamma ray; API—standardized unit of the American Petroleum Institute; TWT—two-way travelttime.

the large-scale architecture and stacking pattern of hybrid turbidite-drift channel complexes along the East African margin (Fig. 4B).

CONCLUSIONS

Modern and ancient submarine slope channels offshore of Tanzania and Mozambique are, and were, formed by episodic, unsteady, high-energy but short-duration, east-flowing turbidity current events superimposed on long-lived, quasi-steady, northward-flowing bottom currents. The channels are bordered by hybrid levee-drift deposits on their bottom current-downstream (northern) sides, which step progressively southward. Channels have steep eroded margins on

their bottom current-upstream (southern) side, and gently dipping downstream flanks where the drift-levees step into the channel. We relate the upstream-migrating levee-drifts to lee-wave conditions as bottom currents traverse the channel. The continued development of the drift-levee pins the channels to the slope for protracted time periods. Well core data indicate that the "toes" of the drift stepping into the channel are dominantly finely laminated siltstones, and that the internal channel architecture and facies distributions are strongly controlled by turbidity- and bottom-current interaction. Our integrated study is likely applicable to many other drift systems globally, and provides new quantitative data to

Figure 4. (A) Sedimentological model of hybrid levee-drift systems: i—with concurrent gravity-driven turbidity currents; ii—during dominance of bottom currents. Red arrow represents turbidity current; blue arrows represent bottom current. (B) Laterally offset channel complexes after repeated intervals of bottom current-dominated and turbidity current-dominated deposition. (C) Graphic visualization of the spatial variation of turbidity currents and bottom-current flows over time. Velocity (U) values are taken from published work (Tables DR2 and DR3 [see footnote 1]) and bottom-current measurements offshore of Mozambique (Fig. 2; see footnote 1).

enable the inference of bottom-current direction from ancient sedimentary sequences, which can be applied to existing and future studies.

ACKNOWLEDGMENTS

We thank Michal Janocko for assistance with data analysis, and acknowledge the helpful reviews of F. Gamberi, F.J. Hernandez-Molina, and G. Shanmugam. We acknowledge funding and data supplied by Equinor ASA, and data from Eni energy company and from ExxonMobil. Clare was supported by the Climate Linked Atlantic Sector Science (CLASS) programme (Natural Environment Research Council Grant No. NE/R015953/1).

REFERENCES CITED

- Azpiroz-Zabala, M., Cartigny, M.J.B., Talling, P.J., Parsons, D.R., Sumner, E.J., Clare, M.A., Simmons, S.M., Cooper, C., and Pope, E.L., 2017, Newly recognized turbidity current structure can explain prolonged flushing of submarine canyons: *Science Advances*, v. 3, e1700200, <https://doi.org/10.1126/sciadv.1700200>.
- Clare, M.A., Hughes Clarke, J.E., Talling, P.J., Cartigny, M.J.B., and Pratomo, D.G., 2016, Preconditioning and triggering of offshore slope failures and turbidity currents revealed by most detailed monitoring yet at a fjord-head delta: *Earth and Planetary Science Letters*, v. 450, p. 208–220, <https://doi.org/10.1016/j.epsl.2016.06.021>.
- de Ruijter, W.P.M., Ridderinkhof, H., Lutjeharms, J.R.E., Schouten, M.W., and Veth, C., 2002, Observations of the flow in the Mozambique Channel: *Geophysical Research Letters*, v. 29, p. 1401–1403, <https://doi.org/10.1029/2001gl013714>.
- Drinkorn, C., Saynisch-Wagner, J., Uenzelmann-Neben, G., and Thomas, M., 2019, Transport, Removal and Accumulation of sediments Numerically Simulated for Paleo-Oceans and Reconstructed from cores of The Eirik Drift (TRANSPORTED): Abstract presented at International Ocean Discovery Program–International Continental Scientific Drilling Program Kollquium, Cologne, Germany, 18–20 March.
- Faugères, J.-C., Stow, D.A., Imbert, P., and Viana, A., 1999, Seismic features diagnostic of contourite drifts: *Marine Geology*, v. 162, p. 1–38, [https://doi.org/10.1016/S0025-3227\(99\)00068-7](https://doi.org/10.1016/S0025-3227(99)00068-7).
- Fierens, R., Droz, L., Toucanne, S., Raison, F., Jouet, G., Babonneau, N., Miramontes, E., Landurain, S., and Jorry, S.J., 2019, Late Quaternary geomorphology and sedimentary processes in the Zambesi turbidite system (Mozambique Channel): *Geomorphology*, v. 334, p. 1–28, <https://doi.org/10.1016/j.geomorph.2019.02.033>.
- Flood, R.D., 1988, A lee wave model for deep-sea mud-wave activity: *Deep-Sea Research: Part A, Oceanographic Research Papers*, v. 35, p. 973–983, [https://doi.org/10.1016/0198-0149\(88\)90071-4](https://doi.org/10.1016/0198-0149(88)90071-4).
- Fonnesu, M., Palermo, D., Galbiati, M., Marchesini, M., Bonamini, E., and Bendias, D., 2020, A new world-class deep-water play-type, deposited by the syndepositional interaction of turbidity flows and bottom currents: The giant Eocene Coral Field in northern Mozambique: *Marine and Petroleum Geology*, v. 111, p. 179–201, <https://doi.org/10.1016/j.marpetgeo.2019.07.047>.
- Fossum, K., Morton, A.C., Dypvik, H., and Hudson, W.E., 2019, Integrated heavy mineral study of Jurassic to Paleogene sandstones in the Mandawa Basin, Tanzania: Sediment provenance and source-to-sink relations: *Journal of African Earth Sciences*, v. 150, p. 546–565, <https://doi.org/10.1016/j.jafrearsci.2018.09.009>.
- Gamberi, F., Rovere, M., Dykstra, M., Kane, I.A., and Kneller, B.C., 2013, Integrating modern seafloor and outcrop data in the analysis of slope channel architecture and fill: *Marine and Petroleum Geology*, v. 41, p. 83–103, doi: <https://doi.org/10.1016/j.marpetgeo.2012.04.002>.
- Gong, C., Wang, Y., Rebesco, M., Salon, S., and Steel, R.J., 2018, How do turbidity flows interact with contour currents in unidirectionally migrating deep-water channels?: *Geology*, v. 46, p. 551–554, <https://doi.org/10.1130/G40204.1>.
- Hubbard, S.M., Covault, J.A., Fildani, A., and Romans, B.W., 2014, Sediment transfer and deposition in slope channels: Deciphering the record of enigmatic deep-sea processes from outcrop: *Geological Society of America Bulletin*, v. 126, p. 857–871, <https://doi.org/10.1130/B30996.1>.
- Kane, I.A., and Clare, M.A., 2019, Dispersion, accumulation, and the ultimate fate of microplastics in deep-marine environments: A review and future directions: *Frontiers of Earth Science*, v. 7, 80, <https://doi.org/10.3389/feart.2019.00080>.
- Martín-Chivelet, J., Fregenal-Martínez, M.A., and Chacón, B., 2008, Traction structures in contourites, in Rebesco, M., and Camerlenghi, A., eds., *Contourites: Amsterdam, Elsevier Science, Developments in Sedimentology*, v. 60, p. 159–182, [https://doi.org/10.1016/S0070-4571\(08\)10010-3](https://doi.org/10.1016/S0070-4571(08)10010-3).
- Masson, D.G., Huvenne, V.A.I., de Stigter, H.C., Wolff, G.A., Kiriakoulakis, K., Arzola, R.G., and Blackbird, S., 2010, Efficient burial of carbon in a submarine canyon: *Geology*, v. 38, p. 831–834, <https://doi.org/10.1130/G30895.1>.
- Miramontes, E., et al., 2019, The influence of bottom currents on the Zambesi Valley morphology (Mozambique Channel, SW Indian Ocean): In situ current observations and hydrodynamic modeling: *Marine Geology*, v. 410, p. 42–55, <https://doi.org/10.1016/j.margeo.2019.01.002>.
- Nauw, J.J., van Aken, H.M., Webb, A., Lutjeharms, J.R.E., and de Ruijter, W.P.M., 2008, Observations of the southern East Madagascar Current and undercurrent and countercurrent system: *Journal of Geophysical Research*, v. 113, C08006, <https://doi.org/10.1029/2007JC004639>.
- Palermo, D., Galbiati, M., Famiglietti, M., Marchesini, M., Mezzapesa, D., and Fonnesu, F., 2014, Insights into a new super-giant gas field—Sedimentology and reservoir modeling of the Coral Reservoir Complex, offshore northern Mozambique: Paper presented at Offshore Technology Conference—Asia, Kuala Lumpur, Malaysia, 25–28 March, <https://doi.org/10.4043/24907-MS>.
- Rebesco, M., Hernández-Molina, F.J., Van Rooij, D., and Wählin, A., 2014, Contourites and associated sediments controlled by deep-water circulation processes: State-of-the-art and future considerations: *Marine Geology*, v. 352, p. 111–154, <https://doi.org/10.1016/j.margeo.2014.03.011>.
- Reeves, C.V., 2018, The development of the East African margin during Jurassic and Lower Cretaceous times: A perspective from global tectonics: *Petroleum Geoscience*, v. 24, p. 41–56, <https://doi.org/10.1144/petgeo2017-021>.
- Reeves, C.V., Teasdale, J.P., and Mahanjane, E.S., 2016, Insight into the East Coast of Africa from a new tectonic model of the early Indian Ocean, in Nemčok, M., et al., eds., *Transform Margins: Development, Controls and Petroleum Systems: Geological Society [London] Special Publication 431*, p. 299–322, <https://doi.org/10.1144/SP431.12>.
- Salman, G., and Abdula, I., 1995, Development of the Mozambique and Ruvuma sedimentary basins, offshore Mozambique: *Sedimentary Geology*, v. 96, p. 7–41, [https://doi.org/10.1016/0037-0738\(95\)00125-R](https://doi.org/10.1016/0037-0738(95)00125-R).
- Sansou, P., 2018, Hybrid turbidite–contourite systems of the Tanzanian margin: *Petroleum Geoscience*, v. 24, p. 258–276, <https://doi.org/10.1144/petgeo2018-044>.
- Schouten, M.W., De Ruijter, W.P.M., van Leeuwen, P.J., and Ridderinkhof, H., 2003, Eddies and variability in the Mozambique Channel: *Deep-Sea Research: Part II, Topical Studies in Oceanography*, v. 50, p. 1987–2003, [https://doi.org/10.1016/S0967-0645\(03\)00042-0](https://doi.org/10.1016/S0967-0645(03)00042-0).
- Shanmugam, G., Spalding, T.D., and Rofheart, D.H., 1993, Process sedimentology and reservoir quality of deep-marine bottom-current reworked sands (sandy contourites): An example from the Gulf of Mexico: *American Association of Petroleum Geologists Bulletin*, v. 77, p. 1241–1259, <https://doi.org/10.1306/BDF8E52-1718-11D7-8645000102C1865D>.
- Smelror, M., Key, R.M., Smith, R.A., and Njange, F., 2008, Late Jurassic and Cretaceous palynostratigraphy of the onshore Rovuma Basin, Northern Mozambique: *Palynology*, v. 32, p. 63–76, <https://doi.org/10.2113/gspalynol.32.1.63>.
- Sømme, T.O., Helland-Hansen, W., Martinsen, O.J., and Thurmond, J.B., 2009, Relationships between morphological and sedimentological parameters in source-to-sink systems: A basis for predicting semi-quantitative characteristics in subsurface systems: *Basin Research*, v. 21, p. 361–387, <https://doi.org/10.1111/j.1365-2117.2009.00397.x>.
- Stow, D.A.V., and Faugères, J.-C., 2008, Contourite facies and the facies model, in Rebesco, M., and Camerlenghi, A., eds., *Contourites: Amsterdam, Elsevier Science, Developments in Sedimentology*, v. 60, p. 223–256, [https://doi.org/10.1016/S0070-4571\(08\)10013-9](https://doi.org/10.1016/S0070-4571(08)10013-9).
- Stow, D.A.V., Hernández-Molina, F.J., Llave, E., Sayago-Gil, M., Díaz del Río, V., and Branson, A., 2009, Bedform-velocity matrix: The estimation of bottom current velocity from bedform observations: *Geology*, v. 37, p. 327–330, <https://doi.org/10.1130/G25259A.1>.
- Symons, W.O., Sumner, E.J., Paull, C.K., Cartigny, M.J.B., Xu, J.P., Maier, K.L., Lorenson, T.D., and Talling, P.J., 2017, A new model for turbidity current behavior based on integration of flow monitoring and precision coring in a submarine canyon: *Geology*, v. 45, p. 367–370, <https://doi.org/10.1130/G38764.1>.
- Talling, P.J., Masson, D.G., Sumner, E.J., and Magesini, G., 2012, Subaqueous sediment density flows: Depositional processes and deposit types: *Sedimentology*, v. 59, p. 1937–2003, <https://doi.org/10.1111/j.1365-3091.2012.01353.x>.
- Thiéblemont, A., Hernández-Molina, F.J., Miramontes, E., Raison, F., and Penven, P., 2019, Contourite depositional systems along the Mozambique channel: The interplay between bottom currents and sedimentary processes: *Deep-Sea Research: Part I, Oceanographic Research Papers*, v. 147, p. 79–99, <https://doi.org/10.1016/j.dsr.2019.03.012>.
- Thran, A.C., Dutkiewicz, A., Spence, P., and Müller, R.D., 2018, Controls on the global distribution of contourite drifts: Insights from an eddy-resolving ocean model: *Earth and Planetary Science Letters*, v. 489, p. 228–240, <https://doi.org/10.1016/j.epsl.2018.02.044>.
- van Aken, H.M., Ridderinkhof, H., and de Ruijter, W.P.M., 2004, North Atlantic deep water in the south-western Indian Ocean: *Deep-Sea Research: Part I, Oceanographic Research Papers*, v. 51, p. 755–776, <https://doi.org/10.1016/j.dsr.2004.01.008>.
- Vendettuoli, D., et al., 2019, Daily bathymetric surveys document how stratigraphy is built and its extreme incompleteness in submarine channels: *Earth and Planetary Science Letters*, v. 515, p. 231–247, <https://doi.org/10.1016/j.epsl.2019.03.033>.

Printed in USA